Journal of Electroanalytical Chemistry 997 (2025) 119500

Contents lists available at ScienceDirect

Journal of Electroanalytical Chemistry

journal homepage: www.elsevier.com/locate/jelechem

Facile electrochemical assay of thrombin activity in biological products

Wan-Yue Zhuang [a], Zi-Yi Wang [a], Xingdong Yang [a], Jun-Qin Qiao [a,*], Wei-Juan Zheng [b], Hong-Zhen Lian [a,*]

[a] State Key Laboratory of Analytical Chemistry for Life Science, School of Chemistry & Chemical Engineering and Centre for Shared Scientific Research Facilities, Nanjing University, 163 Xianlin Avenue, Nanjing 210023, China
[b] State Key Laboratory of Pharmaceutical Biotechnology, School of Life Sciences, Nanjing University, 163 Xianlin Avenue, Nanjing 210023, China

ARTICLE INFO

Keywords:
Thrombin
Activity
Peptide
Biological product
Electrochemical detection

ABSTRACT

Thrombin, a critical protein-based therapeutic agent, is widely used in modern medicine. Precise quantification of thrombin enzymatic activity represents a fundamental requirement for both manufacturing quality control and clinical therapeutic monitoring. Here, we developed a "signal-off" electrochemical method for the rapid detection of thrombin activity within 15 min. A thrombin-specific substrate peptide was anchored to a gold electrode via Au—S bonds at its C-terminal, with an N-terminal ferrocene (Fc) tag as a redox probe. A cellulose acetate (CA) membrane was added to reduce contamination and signal loss. The detection mechanism relies on thrombin-mediated peptide cleavage, detaching the Fc-tagged fragment and generates a decreasing current proportionally to enzyme activity. The detection limit of the described method is 81.1 U/mL, with a linear response over the range of 200–1500 U/mL ($R^2 = 0.9941$), satisfying the quality control requirements for commercial thrombin drugs. This biosensing strategy combines operational simplicity with analytical reliability, showing significant potential for rapid and efficient assessment of thrombin biological products activity.

1. Introduction

Protein therapeutics represent a crucial class of treatments in modern medicine [1–3]. According to the functions of proteins, they are generally classified into therapeutic proteins with regulatory activities such as enzymes [4] and hormones [5], therapeutic proteins with targeting specificity such as monoclonal antibodies [6], protein vaccines such as hepatitis B vaccine [7] and diagnostic proteins such as imaging agents [8]. Among them, enzyme-based drugs are gaining significant attention for their unique ability to catalyze biochemical reactions with high specificity toward target molecules. Thrombin, a serine protease, serves as an essential enzyme in the coagulation cascade by cleaving soluble fibrinogen into insoluble fibrin, thereby facilitating stable clot formation [9]. Beyond clotting, thrombin also activates cell signals via protease-activated receptors (PARs), thereby promoting blood vessel growth and tissue repair [10,11]. In recent years, thrombin has been widely used as a fast-acting local hemostasis drug in surgery. The efficacy and safety of thrombin drugs is correlated with their enzymatic activity. Thrombin with insufficient activity cannot achieve good therapeutic efficacy, while its application at excessively high activity levels may cause thrombosis or worsen inflammation [12–14]. Additionally, due to protein's instability, the activity of thrombin drugs is susceptible to alteration by environmental factors. More importantly, in urgent clinical scenarios where thrombin must be administered immediately to control life-threatening bleeding, there is no time to wait for lengthy laboratory testing. Consequently, facile and accurate on-site thrombin activity assessment is critical for rapid screening of final product, stability monitoring throughout storage and distribution chains, and especially for point-of-care to balance treatment benefits and risks, ensuring patient safety.

In industry, the monitoring of thrombin activity is based on pharmacopoeia standards. They are mainly divided into two categories: one is the clotting time assay which monitors the clotting time of fibrinogen under the reaction with thrombin, and the other is ultraviolet-visible spectrophotometry (UV–Vis) method that detects changes in absorbance of chromogenic substrate before and after hydrolysis. The former method is adopted by the Chinese Pharmacopoeia (ChP) [15], the U.S. Pharmacopoeia (USP) [16] and the Japanese Pharmacopoeia (JP) [17]. The latter method is used in the European Pharmacopoeia (EP) [18]. These methods serve as the gold-standard approaches for in-process control and product release within pharmaceutical manufacturing. However, the sensitivity of clotting time assay method is limited by

* Corresponding authors.
E-mail addresses: qiaojunqin@nju.edu.cn (J.-Q. Qiao), hzlian@nju.edu.cn (H.-Z. Lian).

https://doi.org/10.1016/j.jelechem.2025.119500
Received 26 July 2025; Received in revised form 21 September 2025; Accepted 22 September 2025
Available online 23 September 2025

visual endpoint detection, leading to variability influenced by operator's experience. And the UV–Vis method may be interfered by substrates or matrix in the solution, introducing inaccurate measurements. Literature reported many other methods for detecting thrombin, such as colorimetry [19,20], fluorescence spectrometry [21–23], surface-enhanced Raman spectroscopy (SERS) [24], electrochemiluminescence (ECL) [25,26] and photoelectrochemical techniques [27]. Most of them primarily focused on quantifying thrombin concentration, whereas functional activity evaluation remains underrepresented. In addition, these optical methods could be influenced by environmental interference, leading to inconsistent outcomes.

Electrochemical detection serves as a vital technique in both biological [28,29] and chemical analysis [30]. It has emerged as an important tool for fast, on-site detection of biological molecules, owing to its quick response, small device size, and ability to work with multiple samples [31–35]. These features make it highly valuable for point-of-care testing (POCT) and monitoring drug treatments [36,37]. For example, glucose meters using amperometric detection have greatly changed diabetes management [38]. Research shows that electrochemical method has been employed for detecting thrombin in complex biological samples [39–42]. However, existing electrochemical methods remain unsuitable for thrombin-based biological products. Consequently, there is an urgent need to develop a rapid and reliable method for on-site assessing thrombin activity within biopharmaceuticals.

Regarding the above issues, we developed a "signal-off" electrochemical method for rapid detection of thrombin activity, which is specially applicable to thrombin biological products. The detection system employed screen-printed electrodes (SPEs), which are compact in size, convenient for storage and portability, and do not require electrolytic cells or a large amount of electrolyte. A thrombin-specific substrate peptide was used to quantify enzymatic activity, ensuring method specificity and enhancing the accuracy and reliability of quantification. Very interestingly, the method is easy to operate with high stability, and the entire thrombin activity detection steps can be completed within 15 min.

2. Experimental section

2.1. Materials and reagents

Materials. Screen-printed gold electrodes (SPGEs, model: DRP-C220AT-U75) were purchased from Metrohm China Ltd. (Shanghai, China). The incubator was purchased from Shanghai Lichen Instrument Technology Co., Ltd. (Shanghai, China).

Reagents. The substrate ferrocene modified peptide (Pe-Fc, sequence: Fc-GLVPRGSC) was obtained from Sangon Biotechnology Co. (Shanghai, China) and used without further purification. Thrombin (5000 U) purchased from Nanjing Dulai Biotechnology Co., Ltd. (Nanjing, China) was used for condition optimization. Thrombin certified reference material (CRM) and fibrinogen (CRM) were provided by the National Institutes for Food and Drug Control (NIFDC, Beijing, China). Thrombin testing samples were obtained from commercially available products. Potassium phosphate monobasic (KH_2PO_4), potassium phosphate dibasic (K_2HPO_4), cellulose acetate (CA, acetyl content: 39.8 wt%; hydroxyl content: 3.5 wt%), L-cysteine (L-Cys) and chymotrypsin (Chy) were purchased from Shanghai Aladdin Biochemical Technology Co., Ltd. (Shanghai, China). Potassium chloride (KCl), sodium chloride (NaCl), urea, L-alanine (L-Ala) and hemoglobin (Hb) were acquired from Shanghai Macklin Biochemical Co., Ltd. (Shanghai, China). PNGase F and O-Glycosidase were obtained from New England Biolabs (Ipswich, MA, USA). Human urinary kallidinogenase (HUK) was provided by Aidea Pharmaceutical Co., Ltd. (Yangzhou, China). Acetone (AC, analytical grade) and *N*,*N*-dimethylformamide (DMF, analytical grade) were purchased from Nanjing Chemical Reagent Co., Ltd. (Nanjing, China) and Sinopharm Chemical Reagent Co., Ltd. (Beijing, China), respectively. Tris-HCl buffer (1 M, pH 7.40) was supplied by Beyotime Biotechnology (Shanghai, China). All aqueous solutions were prepared using ultrapure water (18.2 MΩ·cm) purified through a Milli-Q water purification system (Millipore, Billerica, MA, USA). 50 mM Tris-HCl was obtained by dilution. 0.01 M PBS was obtained by preparing 0.01 M K_2HPO_4 and KH_2PO_4 containing 0.01 M KCl respectively, mixing them and adjusting the pH = 7.40.

2.2. Apparatus

Square wave voltammetry (SWV), cyclic voltammetry (CV) and electrochemical impedance spectroscopy (EIS) experiments were performed using a CHI660E electrochemistry workstation (Chenhua, Shanghai, China), equipped with a conventional three-electrode system. EIS was performed at the open circuit potential in 0.1 M KCl containing 5.0 mM $[Fe(CN)_6]^{3-/4-}$ (frequency range: 10^6 Hz to 0.1 Hz, amplitude: 5.0 mV), while CV was acquired in the same electrolyte over a potential window of −0.4 to 0.9 V at a scan rate of 0.05 V/s. Scanning electron microscopy (SEM) images were taken on a Hitachi S4800 microscope (Hitachi, Tokyo, Japan) connected to a Bruker Quantax energy-dispersive spectrometer (EDS, Bruker, Karlsruhe, Germany). The water contact angles of the electrodes were measured using a DSA100 Drop Shape Analyzer (KRÜSS Scientific, Hamburg, Germany). Raman spectra were collected on a Raman spectrometer equipped with a 785 nm laser (LabRAM HR Evolution, HORIBA, France).

2.3. SPGE/Pe-Fc/CA preparation

Screen-printed gold electrodes (SPGEs) were rinsed with ultrapure water prior to functionalization. The cleaned SPGEs were incubated with 10 μL of 1200 μM Pe-Fc solution (0.01 M PBS: 0.01 M K_2HPO_4/KH_2PO_4, 0.01 M KCl, pH 7.40) at 4 °C overnight, followed by thorough rinsing with PBS to remove unbound Pe-Fc. After that, 4 μL of 0.5 % CA solution (AC:DMF = 3:7, v:v) was dropped onto the surface of SPGE/Pe-Fc to form a CA membrane. The SPGE/Pe-Fc/CA was stored in a refrigerator at 4 °C for further use.

2.4. Electrochemical detection of thrombin

The SPGE/Pe-Fc/CA was incubated with 10 μL of thrombin with different concentrations (0.05 M Tris–HCl, pH 7.40) at 37 °C for 10 min. After the extensive washing with Tris–HCl buffer, square wave voltammetry (SWV) measurements were performed in 0.01 M PBS across a potential window of 0 to 0.8 V. The 0.05 M Tris-HCl blank control was subjected to the same procedure as that of thrombin.

3. Results and discussion

3.1. Principle of the electrochemical detection of thrombin activity

The operational principle of the thrombin activity electrochemical detection platform is depicted schematically in Scheme 1. Central of this "signal-off" mechanism lies a thrombin-specific substrate peptide that is directionally immobilized on a gold electrode surface. This orientation-controlled assembly is achieved through covalent Au—S bonds formed between the electrode and the C-terminal cysteine residue of the peptide. A ferrocene (Fc) tagged on the peptide's N-terminal functions as an electrochemical redox reporter, generating a quantifiable baseline amperometric signal. To reduce interfacial fouling and minimize non-specific signal attenuation in complex media, a nanoporous CA membrane (pore size: 50–200 nm) is engineered onto the electrode surface. Crucially, upon the introduction of thrombin, site-specific proteolytic cleavage occurs at the Arg-Gly scissile bond within the peptide backbone. This enzymatic hydrolysis results in the release of the Fc-tagged fragment into the solution, leading to a decrease in faradaic current. The extent of current decrease is directly correlated with level of thrombin activity.

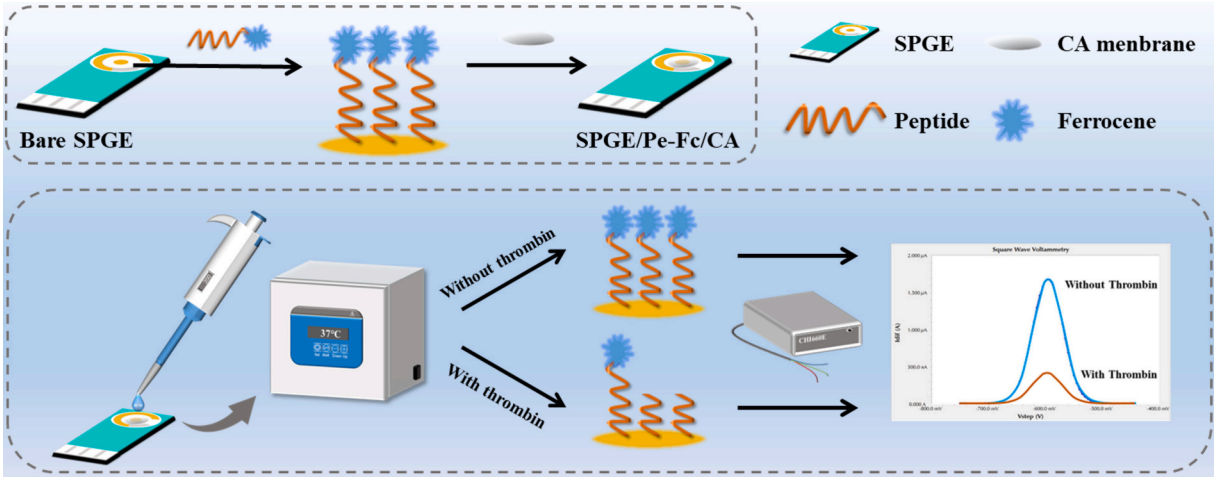

Scheme 1. Principle of the electrochemical detection of thrombin activity.

3.2. Characterization

To investigate the surface morphology of the electrodes, scanning electron microscopy (SEM) was performed. When compared to the bare electrode (Fig. 1A), no significant changes in the surface appearance of SPGE/Pe-Fc were observed as shown in Fig. 1B, likely due to the peptide molecules being too small to be distinctly visualized under SEM. This indicates that the peptide modification does not noticeably affect the electrode's surface characteristics. Differently, upon coating the electrode with a cellulose acetate membrane (Fig. 1C), the surface underwent notable changes.

To further verify the functionalization of peptide onto the electrode surface, we employed energy dispersive X-ray spectroscopy (EDS) for elemental analysis. As shown in Fig. S1, besides Au, the bare SPGE also contained other metal elements such as Al and Na, along with non-metal elements Si, C and O. It is speculated that the other elements come from the ceramic substrate of the screen-printed gold electrode. After modification with the substrate peptide (Fig. S2), the EDS analysis revealed the presence of S and Fe in addition to elements already present on the bare electrode, indicating their incorporation into the SPGE/Pe-Fc surface. This result fits well with the theoretical elemental composition of Pe-Fc (containing H, C, N, O, S, Fe), proving the successful modification of peptides on the SPGE surface. Notably, the appearance of K in the spectrum is likely attributed to residual potassium ions from PBS buffer utilized during the dissolution of the substrate peptide. When the modified electrode was coated with a cellulose acetate membrane, EDS result (Fig. S3) revealed the presence of only C and O besides Au. This is because the membrane physically blocks signals from other elements, demonstrating the successful modification of cellulose acetate membrane.

Water contact angle measurements were employed to characterize the hydrophilicity of the electrode surfaces. As depicted in Fig. S4, the water contact angles for the bare SPGE and SPGE/Pe-Fc were 101.8°and 55.9°, respectively. This indicated that the modification of Pe-Fc changes the electrode surface from hydrophobic to hydrophilic. Notably, the similar water contact angle observed for SPGE/Pe-Fc and SPGE/Pe-Fc/CA suggested that the CA membrane exhibits a hydrophilicity comparable to that of Pe-Fc layer. The change in contact angle further indicated the successful modification of Pe-Fc and CA membrane on the electrode.

Raman spectroscopy was also performed to further characterize the electrode modifications. As shown in Fig. S5, the Raman spectra of the bare SPGE showed no characteristic peaks of organic compounds. After the modification of Pe-Fc, a distinct Au—S band appeared at 146 cm^{-1}, indicating that the peptide was successfully immobilized on the electrode surface. Upon further coating with a CA membrane, new absorption peaks emerged at 1095, 1374, 2897, and 3362 cm^{-1}, which were assigned to C—O stretching, C—H bending, C—H stretching, and O—H stretching vibrations, respectively. These characteristic peaks can be attributed to cellulose acetate, confirming the successful formation of the CA membrane on the electrode. Notably, the peak of Au—S at 146 cm^{-1} remained detectable after CA deposition, suggesting that the CA membrane did not completely block Raman signal from the underlying Au—S bonds, and that the Au—S bonds remained stable under the protective coating.

Using $[Fe(CN)_6]^{3-/4-}$ as the probes, the preparation of the SPGE/Pe-Fc/CA was further characterized using CV and EIS. The CV and Nyquist plots were shown in Fig. 2A-B. For the bare electrode, the highest redox current and smallest charge transfer resistance (R_{ct}) were observed. After modification with the signal molecule-conjugated peptide, the redox current slightly decreased, and as expected, there was a small increase in R_{ct}. This phenomenon can be attributed to the steric hindrance caused by the substrate peptide. Due to the non-conductivity of polymers, the modification of the CA membrane caused a significant

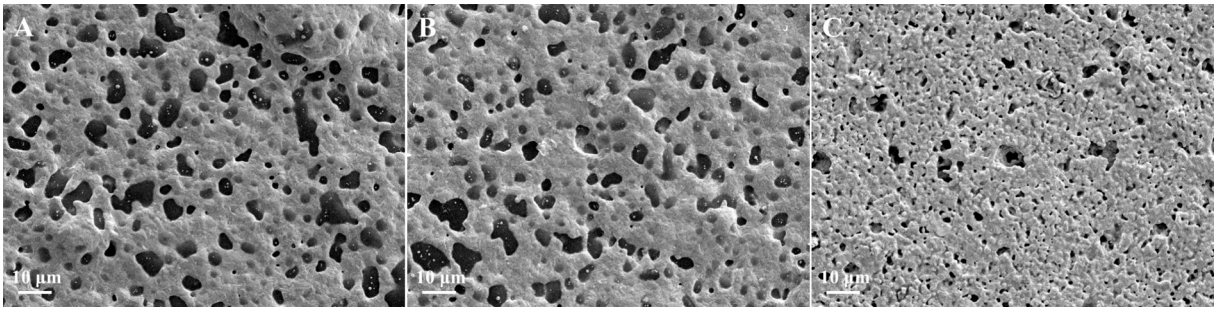

Fig. 1. SEM image of the bare SPGE (A), the SPGE/Pe-Fc (B) and the SPGE/Pe-Fc/CA (C).

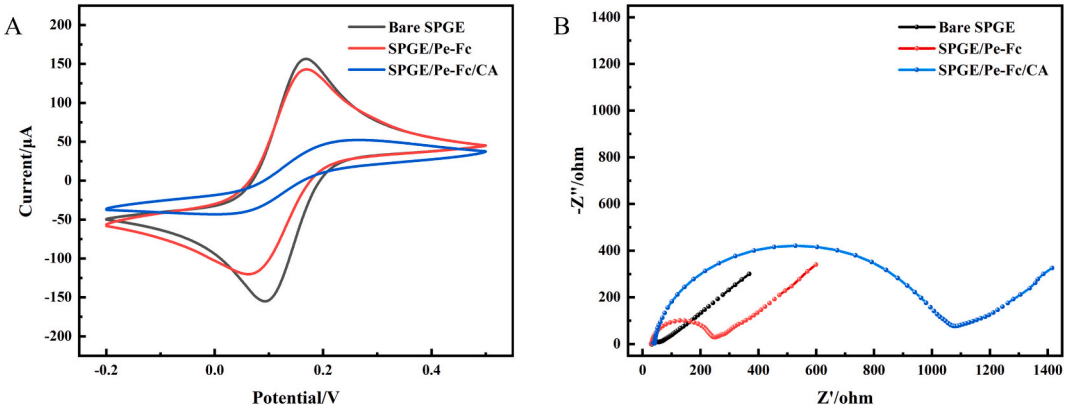

Fig. 2. CV (A) and Nyquist (B) curves of the bare SPGE, SPGE/Pe-Fc and SPGE/Pe-Fc/CA. The supporting electrolyte was 0.1 M KCl containing 5.0 mM $[Fe(CN)_6]^{3-/4-}$.

reduction in redox current, leading to a marked rise in R_{ct}. The variation of the redox current in the cyclic voltammetry (CV) plot exhibits a consistent trend with the alteration of R_{ct} as depicted in the EIS plot, providing strong evidence for the successful preparation of the electrodes.

3.3. Effects of experimental conditions

The application of anti-fouling coatings to the detection system can effectively prevent both surface contamination and signal degradation during the electrode storage [43].

Cellulose acetate (CA), a kind of porous material, can function as an exclusion volume membrane. Besides simplicity and inexpensiveness, it exhibits excellent biocompatibility and high stability [44,45]. Due to these attributes, cellulose acetate membranes have found extensive application [46]. To prevent the detachment of substrate peptides and potential contamination during transportation and storage, a cellulose acetate (CA) membrane was applied to protect the electrode. The impact of CA concentration (ranging from 0.1 % to 1.0 %) on current variation before and after enzymolysis was investigated (Fig. 3A). When the CA concentration did not exceed 0.5 %, the reduction in current signal was maintained close to 3 μA. At a CA concentration of 0.1 %, the signal reduction slightly exceeded 3 μA, likely because the thinner membrane formed by low-concentration CA solution minimally hindered reactions between thrombin and substrate peptides. When the concentration exceeded 0.5 %, the measured current change (Δip) had a significant decrease. This can be attributed to the thicker protective membrane formed by excessive CA, which increases the impedance and impedes the interaction between thrombin molecules and substrate molecules, thereby reducing the signal variation. Consequently, 0.5 % CA was identified as the optimal concentration, striking a balance between the physical robustness of membrane and permissible efficiency of signal transduction.

Substrate concentration plays a vital role in influencing enzyme-catalyzed reactions. Thus, the influence of substrate concentration on signal reduction was studied (Fig. 3B). Experimental findings revealed that at low concentration of Pe-Fc (400 μM), the value of signal decrease was only 0.5 μA. When the concentration of the Pe-Fc gradually increased from 400 to 1200 μM, the current variation also gradually increased. This can be attributed to the fact that the continuous replenishment of the substrate enhanced enzymatic digestion reaction, leading to a greater number of substrate peptides being cleaved by the thrombin. However, the increase was not continuous. When the concentration of Pe-Fc exceeds 1200 μM, thrombin is unable to further cleave additional substrate peptides within a short digestion period (10 min), leading to the attainment of a saturation point where the current variation ceases to increase. Accordingly, the 1200 μM Pe-Fc was used in the following experiments.

3.4. Analytical performance

Under optimized experimental conditions, the established method was evaluated for its performance in the quantification of thrombin activity. As illustrated in Fig. 4A, SWV curves demonstrated a clear correlation with thrombin activity. When there is no thrombin, SWV had the highest peak current, and a concentration-dependent decrease in peak current was observed across the thrombin activity range of 200 U/mL to 1500 U/mL. This relationship can be attributed to thrombin-

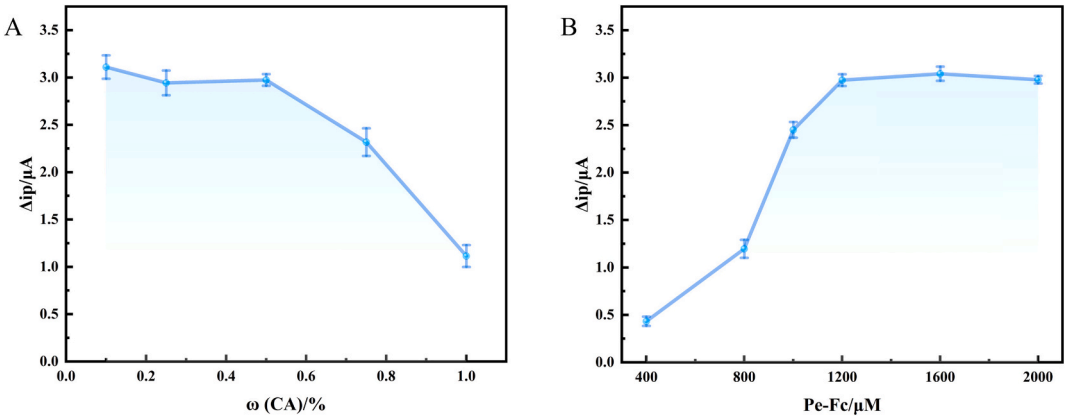

Fig. 3. Effect of the CA concentration (A) and Pe-Fc concentration (B) on current variation ($n = 3$).

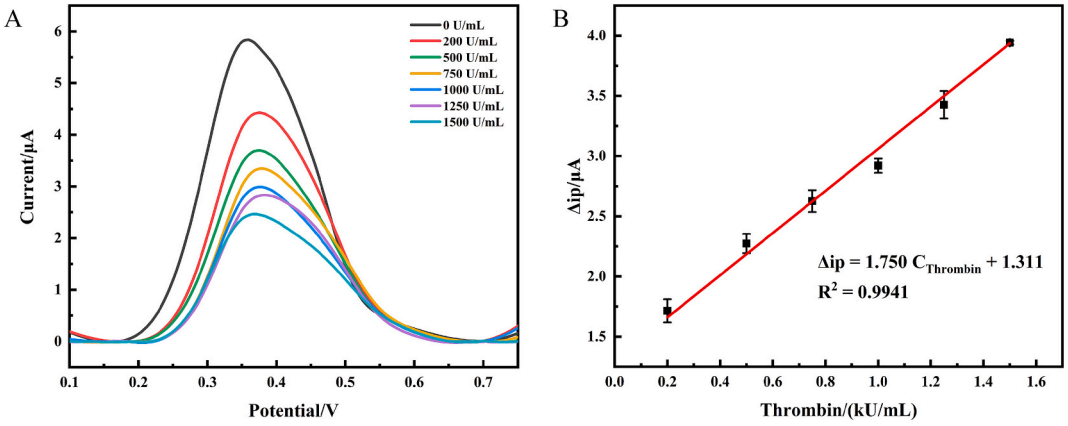

Fig. 4. (A) SWV curves toward various thrombin activities (200–1500 U/mL). (B) The linear relationship between thrombin activity and current variation ($n = 3$).

mediated cleavage of the Fc substrate, where increased enzymatic activity results in greater substrate fragmentation, consequently resulting in gradually reduced peak current. The quantitative relationship between current variation and thrombin activity was shown in Fig. 4B. A strong linear correlation ($R^2 = 0.9941$) was revealed between the Δip and thrombin activity concentration. The calibration equation was $\Delta ip = 1.750\ C_{Thrombin} + 1.311$, where the slope represents the sensitivity of the method. The limit of detection (LOD) was 81.1 U/mL, determined using the 3σ criterion (where σ represents the standard deviation of blank measurements).

The analytical performance of the method was evaluated through comprehensive repeatability studies. Due to the non-reusability of screen-printed electrodes, the evaluation was conducted on different electrodes prepared in the same batch, with the activity concentration of thrombin maintained at 1000 U/mL. The relative standard deviation (RSD) of the current variation among different electrodes after thrombin treatment was 6.0 % (Fig. S6), as measured on the same day. This result suggested satisfactory repeatability between the electrodes. In addition, the consistency of electrode detection performance was evaluated over five consecutive days (Fig. S7), yielding an RSD of 3.1 %, demonstrating the method has good inter-day repeatability.

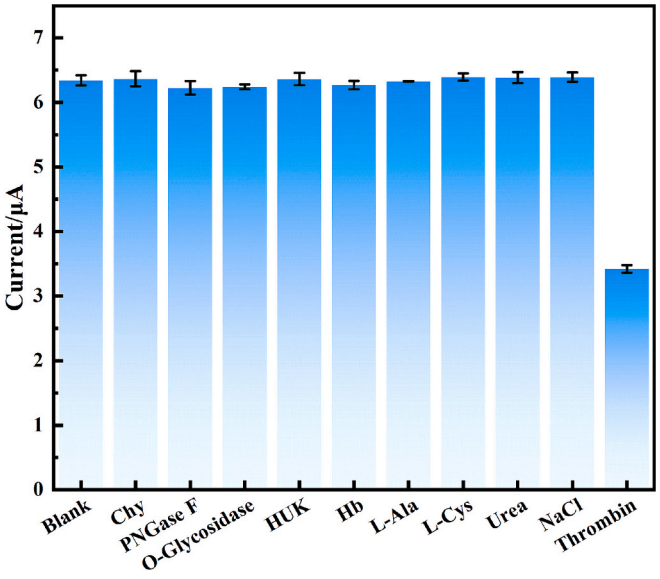

Fig. 5. Peak current corresponding to the addition of interfering substances and 1000 U/mL thrombin ($n = 3$).

3.5. Specificity and storage stability

To systematically evaluate the specificity of the developed method, we investigated potential interfering substances including sodium chloride (NaCl), urea, L-alanine (L-Ala), L-cysteine (L-Cys), hemoglobin (Hb), human urokininase (HUK), O-Glycosidase, PNGase F, and chymotrypsin (Chy). The concentration of these interfering substances was ten times of that of thrombin. As displayed in Fig. 5, the peak current corresponding to the interfering substances was close to that of the background signal (blank measurement), showing no significant interference. In contrast, thrombin cleavage induced a significant decrease in peak current. This result confirms that the method exhibits excellent specificity toward thrombin and can be reliably applied for accurate determination of thrombin activity.

The storage stability of the prepared electrodes (SPGE/Pe-Fc/CA) was evaluated by monitoring changes in current variation before and after enzymatic digestion, over time under different storage conditions. As illustrated in Fig. 6A, during the 14-day storage at 4 °C, the current variations remained at the same level as those of the freshly prepared electrodes. It is demonstrated that the electrodes have comparable performance to freshly prepared electrodes, suggesting the electrodes remain stable for at least 14 days under refrigeration. Furthermore, the electrodes were stored at −20 °C for different days (the longest was 28 days), they also maintained a similar current change level to those of unfrozen controls. These results indicate that the electrodes prepared by the proposed method possess high storage stability, making them suitable for extended use in practical applications.

3.6. Confirmation of the electrochemical method with pharmacopoeia method

To verify the feasibility of the developed method for monitoring thrombin activity in biological products, two types of commercially available thrombin preparations-analytical-grade reagents (1000 U/vial) and lyophilized pharmaceuticals (500 U/vial), were analyzed in parallel using the electrochemical method and the clotting time assay in ChP. As presented in Table 1, the electrochemical approach demonstrated accuracy comparable to the ChP reference method, with all test samples showing similar activity levels between both analytical approaches. To statistically validate these observations, we performed paired *t*-test analysis specifically on thrombin samples with a specified activity of 1000 U/vial. The statistical analysis revealed no significant difference between measurement methods ($t = -0.573$, $p = 0.592 > 0.05$), thereby confirming the reliability of our electrochemical platform for thrombin activity evaluation, further substantiating the platform's reliability for thrombin biologic potency assessment. Notably, our method offers distinct advantages over the ChP protocol. It requires only a simple sample dissolution process, compared to the multi-step

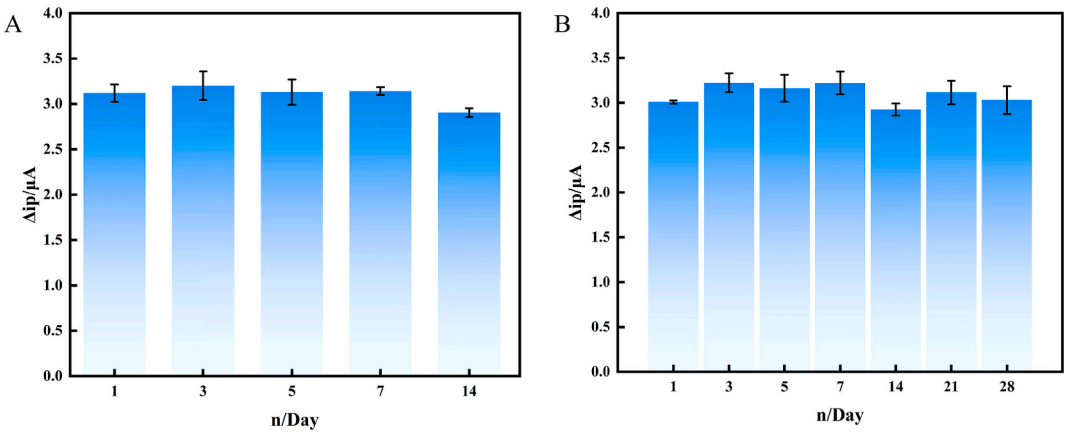

Fig. 6. Storage stability of the fabricated electrodes at 4 °C (A) and − 20 °C (B) (n = 3).

Table 1
Thrombin activity determined by electrochemical and ChP method (n = 3).

No.	Samples	Potency/(U/vial)	
		This work	ChP
1	Thrombin (1000 U/vial)	973.8 ± 38.2	982.6 ± 11.4
2	Thrombin (1000 U/vial)	1078.0 ± 4.0	914.0 ± 6.2
3	Thrombin (1000 U/vial)	903.7 ± 30.0	940.9 ± 8.4
4	Thrombin (1000 U/vial)	1042.1 ± 48.0	962.5 ± 7.0
5	Thrombin (1000 U/vial)	945.8 ± 62.9	938.0 ± 14.6
6	Thrombin (1000 U/vial)	866.5 ± 99.1	948.2 ± 4.6
7	Lyophilizing thrombin powder (500 U/vial)	440.9 ± 30.5	461.8 ± 4.4

preparation steps involved in ChP method. Despite this simplification, our method maintains comparable reproducibility, albeit with slightly elevated measurement variability.

The electrochemical method eliminates the need for visual endpoint determination-a critical requirement in the ChP clotting time measurement, which relies on operators' proficient operating skills and experience. This feature, combined with reduced sample processing requirements and rapid analysis time (<15 min), attributes to establishing the electrochemical methods based on SPGE/Pe-Fc/CA as a robust alternative for rapid quality assessment of thrombin-based biopharmaceuticals.

4. Conclusions

In summary, a "signal-off" electrochemical detection platform was successfully developed using a thrombin-specific substrate peptide as the molecular recognition element, enabling facile thrombin activity detection (detection time < 15 min). The enhanced performance of the platform stems from three key design features: (1) site-specific immobilization of the peptide ensuring molecular orientation control, (2) highly sensitive signal transduction via the ferrocene (Fc) redox reporter system, and (3) significantly improved interference resistance through adding cellulose acetate (CA) protective membranes. Compared to the Pharmacopoeia method, this approach eliminates the need for complex sample pretreatment, while enables on-site and rapid measurement of thrombin functional activity. It provides a technically advanced solution for both quality control in biopharmaceutical production and clinical safety monitoring of thrombin-based therapies.

CRediT authorship contribution statement

Wan-Yue Zhuang: Writing – original draft, Visualization, Validation, Methodology, Investigation, Formal analysis, Data curation. **Zi-Yi Wang:** Methodology, Investigation. **Xingdong Yang:** Methodology, Investigation. **Jun-Qin Qiao:** Writing – review & editing, Validation, Resources, Project administration, Funding acquisition, Formal analysis. **Wei-Juan Zheng:** Supervision, Conceptualization. **Hong-Zhen Lian:** Writing – review & editing, Supervision, Resources, Funding acquisition, Conceptualization.

Declaration of competing interest

The authors declare that they have no known competing financial interests or personal relationships that could have appeared to influence the work reported in this paper.

Acknowledgments

This work was supported by the National Key R&D Program of China (No. 2021YFF0600800), the National Natural Science Foundation of China (22304075, 22176085 and 21874065).

Appendix A. Supplementary data

Supplementary data to this article can be found online at https://doi.org/10.1016/j.jelechem.2025.119500.

References

[1] J.M. Reichert, Trends in development and approval times for new therapeutics in the United States, Nat. Rev. Drug Discov. 2 (9) (2003) 695–702, https://doi.org/10.1038/nrd1178.
[2] B. Leader, Q.J. Baca, D.E. Golan, Protein therapeutics: a summary and pharmacological classification, Nat. Rev. Drug Discov. 7 (1) (2008) 21–39, https://doi.org/10.1038/nrd2399.
[3] Q. Zhu, Z. Chen, P.K. Paul, Y. Lu, W. Wu, J. Qi, Oral delivery of proteins and peptides: challenges, status quo and future perspectives, Acta Pharm. Sin. B 11 (8) (2021) 2416–2448, https://doi.org/10.1016/j.apsb.2021.04.001.
[4] A. Clavell Luis, D. Gelber Richard, J. Cohen Harvey, S. Hitchcock-Bryan, J. R. Cassady, J. Tarbell Nancy, R. Blattner Stephen, R. Tantravahi, P. Leavitt, E. Sallan Stephen, Four-agent induction and intensive asparaginase therapy for treatment of childhood acute lymphoblastic leukemia, N. Engl. J. Med. 315 (11) (1986) 657–663, https://doi.org/10.1056/NEJM198609113151101.
[5] R. Tattersall, Pancretic organotherapy diabetes, 1889-1921, Med. Hist. 39 (3) (1995) 288–316, https://doi.org/10.1017/S0025727300060087.
[6] F. Reicherz, B. Abu-Raya, O. Akinseye, S.R. Rassekh, M.O. Wiens, P.M. Lavoie, Efficacy of palivizumab immunoprophylaxis for reducing severe RSV outcomes in children with immunodeficiencies: a systematic review, J. Pediatr. Infect. Dis. Soc. 13 (2) (2024) 136–143, https://doi.org/10.1093/jpids/piae004.
[7] J. Reutter, P.A. Bart, P. Francioli, A. Safary, P.C. Frei, Production of antibody to hepatitis A virus and hepatitis B surface antigen measured after combined hepatitis

A/ hepatitis B vaccination in 242 adult volunteers, J. Viral Hepat. 5 (3) (1998) 205–211, https://doi.org/10.1046/j.1365-2893.1998.00101.x.
[8] M.J.C. DeHoyos, B.J. Rubal, M.Y.C. Bradley, Detection of acute atrial thrombus in a porcine model with atrial fibrillation with Tc 99m-Apcitide, Investig. Radiol. 39 (4) (2004) 197–201, https://doi.org/10.1097/01.rli.0000112901.01665.e1.
[9] M.W. Mosesson, Fibrinogen and fibrin structure and functions, J. Thromb. Haemost. 3 (8) (2005) 1894–1904, https://doi.org/10.1111/j.1538-7836.2005.01365.x.
[10] G. Luo, C.Y. Wang, J.H. Li, X.C. Zhang, Z.Y. Sun, S. Song, C.Y. Fan, Thrombin improves diabetic wound healing by ERK-dependent and independent Smad2/3 linker region phosphorylation, Curr. Pharm. Des. 28 (17) (2022) 1433–1443, https://doi.org/10.2174/1381612828666220511125237.
[11] R. Catar, G. Moll, I. Hosp, M. Simon, C. Luecht, H. Zhao, D. Wu, L. Chen, J. Kamhieh-Milz, K. Korybalska, D. Zickler, J. Witowski, Transcriptional regulation of thrombin-induced endothelial VEGF induction and proangiogenic response, Cells 10 (4) (2021) 910, https://doi.org/10.3390/cells10040910.
[12] N.A. Shlobin, M. Har-Even, Z.E. Itsekson-Hayosh, S. Harnof, C.G. Pick, Role of thrombin in central nervous system injury and disease, Biomolecules 11 (4) (2021) 562, https://doi.org/10.3390/biom11040562.
[13] E. Mahla, T. Lang, M.N. Vicenzi, G. Werkgartner, R. Maier, C. Probst, H. Metzler, Thromboelastography for monitoring prolonged hypercoagulability after major abdominal surgery, Anesth. Analg. 92 (3) (2001) 572–577, https://doi.org/10.1213/00000539-200103000-00004.
[14] D.J. McCrath, E. Cerboni, R.J. Frumento, A.L. Hirsh, E. Bennett-Guerrero, Thromboelastography maximum amplitude predicts postoperative thrombotic complications including myocardial infarction, Anesth. Analg. 100 (6) (2005) 1576–1583, https://doi.org/10.1213/01.ANE.0000155290.86795.12.
[15] C.P. Commission, Pharmacopoeia of the People's Republic of China, 2020 ed., Beijing, China, 2020.
[16] U.S.P. Convention, United States Pharmacopeia and National Formulary, USP 43–NF, 38 ed., Rockville, MD, USA, 2020.
[17] PMDA, Japanese Pharmacopeia, XVIII ed., Tokoyo, Japan, 2021.
[18] EDQM, European Pharmacopoeia, 10.0th ed., Strasbourg, France, 2019.
[19] G.K. Soni, N. Wangoo, R.K. Sharma, A smartphone-based ultrasensitive colorimetric aptasensing platform for serine protease thrombin detection, Microchem. J. 199 (2024) 109906, https://doi.org/10.1016/j.microc.2024.109906.
[20] M.H. Amani, M. Rahimnejad, H. Ezoji, Smartphone-assisted quantitative colorimetric identification of thrombin based on peroxidase mimetic features of fibrinogen-gold nanozymes, Microchim. Acta 191 (2) (2024) 83, https://doi.org/10.1007/s00604-023-06173-4.
[21] X. Jiang, Y. Li, H. Liu, Q. Zhang, D. Li, W. Zhu, Y. He, G. Zhang, Y. Zhao, Carbon dots doped with nitrogen as an ultrasensitive fluorescent probe for thrombin activity monitoring and inhibitor screening, Talanta 259 (2023) 124532, https://doi.org/10.1016/j.talanta.2023.124532.
[22] Y. Zhang, E. Ranaei Pirmardan, A. Barakat, A. Hafezi-Moghadam, Breath biopsy reveals systemic immunothrombosis and its resolution through bioorthogonal dendritic nanoprobes, Adv. Mater. 35 (45) (2023) 2304903, https://doi.org/10.1002/adma.202304903.
[23] X. Gao, B. Hu, Z. Zhao, T. Niu, Y. Liu, K. Xu, B. Tang, Synthesis of AuSe bonded nanoprobe for specific detection of thrombin in lung cancer cells, Sensors Actuators B Chem. 352 (2022) 130999, https://doi.org/10.1016/j.snb.2021.130999.
[24] P. Anantha, P. Raj, P. Zheng, S. Tanwar, I. Barman, Gold nanoprism enhanced SERS aptasensor for simultaneous detection of thrombin and VEGF, Sensors Actuators B Chem. 423 (2025) 136811, https://doi.org/10.1016/j.snb.2024.136811.
[25] J. Zhang, D. Xu, Z. Deng, X. Tan, D. Guo, Y. Qiao, Y. Li, X. Hou, S. Wang, J. Zhang, Using tungsten oxide quantum-dot enhanced electrochemiluminescence to measure thrombin activity and screen its inhibitors, Talanta 267 (2024) 125267, https://doi.org/10.1016/j.talanta.2023.125267.
[26] D. Xu, Y. Wang, J. Zhang, X. Tan, D. Guo, S. Wang, X. Hou, Simple and low-cost thrombin activity assay using screen-printed electrodes with portable electrochemiluminescence device, Microchem. J. 207 (2024) 112147, https://doi.org/10.1016/j.microc.2024.112147.
[27] M. Gu, X. Yu, Q. Zhou, X. Wu, J. Wang, G.-L. Wang, Biocascade-inspired amplified oxygen vacancy effect on facet-engineered BiOI for ultrasensitive photoelectrochemical detection of 8-oxoguanine DNA glycosylase, Biosens. Bioelectron. 281 (2025) 117466, https://doi.org/10.1016/j.bios.2025.117466.
[28] S. Cui, F. Wang, W. Yang, Highly sensitive electrochemical PDGF-BB sensor based on protein-templated split aptamer ligation reaction, Sensors Actuators B Chem. 425 (2025) 136996, https://doi.org/10.1016/j.snb.2024.136996.
[29] A. Idili, C. Parolo, R. Alvarez-Diduk, A. Merkoçi, Rapid and efficient detection of the SARS-CoV-2 spike protein using an electrochemical aptamer-based sensor, ACS Sensors 6 (8) (2021) 3093–3101, https://doi.org/10.1021/acssensors.1c01222.
[30] X. Luo, S. Cui, W. Yang, Y. Yu, An electrochemical quinine detection approach based on small molecule promoted split aptamer click ligation reaction, Talanta 292 (2025) 127916, https://doi.org/10.1016/j.talanta.2025.127916.
[31] T.-W. Chen, U. Rajaji, S.-M. Chen, A. Muthumariyappan, M.M.A. Mogren, R. Jothi Ramalingam, M. Hochlaf, Facile synthesis of copper(II) oxide nanospheres covered on functionalized multiwalled carbon nanotubes modified electrode as rapid electrochemical sensing platform for super-sensitive detection of antibiotic, Ultrason. Sonochem. 58 (2019) 104596, https://doi.org/10.1016/j.ultsonch.2019.05.013.
[32] S. Yang, F. Yang, W. Dou, Y. Chi, Y. Chi, Testing adulterated liquid-egg: developing rapid detection techniques based on colorimetry, electrochemistry, and interfacial fingerprinting, Food Chem. 444 (2024) 138674, https://doi.org/10.1016/j.foodchem.2024.138674.
[33] Y.F. Fan, Y. Liao, Z.Y. Gao, H.R. Wang, Y. Li, C. Shi, C.P. Ma, N-doped porous carbon synergistic freezing-induced DNA with catalyzed hairpin assembly enables electrochemical one-pot detection of pathogen in food samples, J. Agric. Food Chem. 73 (7) (2025) 4342–4352, https://doi.org/10.1021/acs.jafc.4c11487.
[34] L. Li, F. Tian, F. Wu, L. Qiu, S. Geng, M. Li, Z. Chen, W. Yang, Y. Liu, Y. Yu, Strong electronic metal-support interaction of Ni_4Mo/N-$SrMoO_4$ promotes alkaline hydrogen electrocatalysis, Appl. Catal. B Environ. Energy 361 (2025) 124660, https://doi.org/10.1016/j.apcatb.2024.124660.
[35] X. Ren, L. Qiu, M. Li, F. Tian, L. He, X. Guo, F. Wu, Y. Liu, J. Sheng, W. Yang, Y. Yu, Hierarchically interfacial sulfide/phosphides achieve industry-level water electrolyzer in alkaline conditions at 3 A cm^{-2}, Appl. Catal. B Environ. Energy 378 (2025) 125622, https://doi.org/10.1016/j.apcatb.2025.125622.
[36] C. Ye, D. Shi, Y. Zhu, P. Shi, N. Zhao, Z. Sun, Z. Zhang, D. Zhang, Y. Lv, W. Wu, J. Yu, H. Karimi-Maleh, H. Li, L. Fu, N. Jiang, J. Liu, C.-T. Lin, Graphene electrochemical biosensors combining effervescent solid-phase extraction (ESPE) for rapid, ultrasensitive, and simultaneous determination of DA, AA, and UA, Biosens. Bioelectron. 268 (2025) 116899, https://doi.org/10.1016/j.bios.2024.116899.
[37] W. Lu, X. Xie, X. Lan, P. Wu, H. Peng, J. He, L. Zhong, X. Liu, Z. Deng, Z. Tan, A. Wu, L. Shi, Y. Huang, An electrochemical immunosensor for the detection of Glypican-3 based on enzymatic ferrocene-tyramine deposition reaction, Biosens. Bioelectron. 225 (2023) 115081, https://doi.org/10.1016/j.bios.2023.115081.
[38] L. Zhang, C. Gu, H. Ma, L. Zhu, J. Wen, H. Xu, H. Liu, L. Li, Portable glucose meter: trends in techniques and its potential application in analysis, Anal. Bioanal. Chem. 411 (1) (2019) 21–36, https://doi.org/10.1007/s00216-018-1361-7.
[39] Q. Hu, Y. Bao, S. Gan, Y. Zhang, D. Han, L. Niu, Amplified electrochemical biosensing of thrombin activity by RAFT polymerization, Anal. Chem. 92 (4) (2020) 3470–3476, https://doi.org/10.1021/acs.analchem.9b05647.
[40] Y. Wang, J. Wang, R. Wang, Y. Liu, G.I.N. Waterhouse, X. Ding, V. Raghavan, Single aptamer hairpin DNA-based response system combined with COF-based signal amplification strategy for ultrasensitive detection of cancer-associated thrombin, Chem. Eng. J. 489 (2024) 151224, https://doi.org/10.1016/j.cej.2024.151224.
[41] Y. Feng, G. Liu, F. Zhang, J. Liu, M. La, N. Xia, A General, label-free and homogeneous electrochemical strategy for probing of protease activity and screening of inhibitor, Micromachines 13 (5) (2022) 803, https://doi.org/10.3390/mi13050803.
[42] H. Gong, C. Bao, X. Guo, F. Tian, L. Qiu, W. Yang, A universal electrochemical sensor for detection of nucleic acids and protein based on host-guest recognition of β-cyclodextrin polymer, Microchem. J. 204 (2024) 110987, https://doi.org/10.1016/j.microc.2024.110987.
[43] H. Yang, Q. Hou, C. Ding, Denatured bovine serum albumin hydrogel–based electrochemical biosensors for detection of IgG, Microchim. Acta 189 (11) (2022) 400, https://doi.org/10.1007/s00604-022-05499-9.
[44] M. Woźniak-Budych, U. Zgórzyńska, Ł. Przysiecka, K. Załęski, M. Jarek, M. Jancelewicz, A. Domke, I. Iatsunskyi, G. Nowaczyk, K. Staszak, D. Wieczorek, B. Tylkowski, Copper oxide(I) nanoparticle-modified cellulose acetate membranes with enhanced antibacterial and antifouling properties, Environ. Res. 252 (2024) 119068, https://doi.org/10.1016/j.envres.2024.119068.
[45] B. Yavuzturk Gul, E. Pekgenc, V. Vatanpour, I. Koyuncu, A review of cellulose-based derivatives polymers in fabrication of gas separation membranes: recent developments and challenges, Carbohydr. Polym. 321 (2023) 121296, https://doi.org/10.1016/j.carbpol.2023.121296.
[46] X.J. Hu, T.T. Li, L. Yang, Y. Zhang, B.L. Shen, H.T. Ren, J.H. Lin, C.W. Lou, Optimization, synthesis, and characterization of co-electrospinning cellulose acetate/thermoplastic polyurethanes composite membrane for photodynamic antibacterial application, Cellulose 30 (18) (2023) 11701–11720, https://doi.org/10.1007/s10570-023-05572-3.